

RANDOM LABEL PREDICTION HEADS FOR STUDYING AND CONTROLLING MEMORIZATION IN DEEP NEURAL NETWORKS

006 **Anonymous authors**

007 Paper under double-blind review

ABSTRACT

013 We introduce a straightforward yet effective method to empirically measure and
 014 regularize memorization in deep neural networks for classification tasks. Our
 015 approach augments each training sample with auxiliary random labels, which
 016 are then predicted by a random label prediction head (RLP-head). RLP-heads
 017 can be attached at arbitrary depths of a network, predicting random labels from
 018 the corresponding intermediate representation and thereby enabling analysis of
 019 how memorization capacity evolves across layers. By interpreting the RLP-head
 020 performance as an empirical estimate of Rademacher complexity, we obtain a direct
 021 measure of both sample-level memorization and model capacity. We leverage
 022 this random label accuracy metric to analyze generalization and overfitting in
 023 different models and datasets. Building on this approach, we further propose
 024 a novel regularization technique based on the output of the RLP-head, which
 025 demonstrably reduces memorization. Interestingly, our experiments reveal that
 026 reducing memorization can either improve or impair generalization, depending on
 027 the dataset and training setup. These findings challenge the traditional assumption
 028 that overfitting is equivalent to memorization and suggest new hypotheses to
 029 reconcile these seemingly contradictory results.

1 INTRODUCTION

031 Modern deep learning models are prone to overfitting due to their extreme over-parameterization
 032 (Nakkiran et al., 2021). A wide range of strategies have been proposed to mitigate this issue, including
 033 data augmentation, explicit regularization, and dataset scaling. Although enlarging training datasets
 034 has proven particularly effective, this approach is often infeasible in domains where data acquisition
 035 or annotation is expensive or requires significant human expertise. Moreover, existing strategies
 036 primarily address practical concerns of generalization but provide limited insight into the mechanisms
 037 by which overfitting arises.

038 Recent work highlights the striking memorization capacity of state-of-the-art models. For instance,
 039 Zhang et al. (2021) demonstrate that modern architectures can perfectly fit datasets with randomly
 040 assigned labels, thereby achieving 100 % training accuracy in the absence of any learnable structure.
 041 In such cases, high accuracy is attainable only through memorization of individual training samples,
 042 underscoring that contemporary artificial neural networks (ANNs) can encode sample-specific and
 043 task-irrelevant information to fit each training sample individually.

044 This ability to memorize arbitrary labels is directly connected to the model complexity. In particular,
 045 training with SGD on random labels empirically approximates Rademacher complexity, which plays
 046 a central role in deriving generalization bounds within the PAC-learning framework.

047 The primary objective of this work is to assess the accuracy of predicting random labels as a practical
 048 metric of memorization. Although direct training on random labels reveals a model’s ability to
 049 memorize, this procedure does not intrinsically inform how memorization interacts with generalization
 050 in real-world tasks and does not allow memorization mitigation. To bridge this gap, we propose a
 051 hybrid approach: we augment the network with an additional Random Label Prediction Head (RLP-
 052 head), attached to the feature extractor (i.e., all layers except the final classification layer) in parallel to
 053 the original task head, which remains unchanged. This design enables simultaneous measurement and

054 regularization of memorization during normal training, thereby providing a controlled way to study
 055 and modulate memorization in deep neural networks. In summary, our contribution is as follows:
 056

- 057 • We propose the use of random label prediction heads (RLP-heads) as a tool for probing
 058 layer-wise memorization in deep neural networks.
- 059 • We validate that the random label accuracy derived from RLP-heads is an accurate measure
 060 for complexity and memorization.
- 061 • We propose a novel regularizer that explicitly constrains memorization by penalizing the
 062 performance of the RLP-head during training.
- 063 • Building on our metric and regularizer, we show how memorization can hinder or, in certain
 064 scenarios, facilitate generalization. We further hypothesize that this dual role is driven by
 065 sampling effects in the training data.

067 2 RELATED WORK

070 The phenomenon of data memorization, although not new, gained renewed attention in the era of
 071 modern deep learning with the works of Zhang et al. (2021) and Arpit et al. (2017). Traditionally,
 072 memorization was associated with model capacity and overfitting, and hence viewed primarily as
 073 a source of poor generalization. This view of capacity being responsible for overfitting has been
 074 challenged by the discovery of the double descent phenomenon (Nakkiran et al., 2021), which reveals
 075 a more nuanced relationship between capacity and generalization.

076 Feldman (2019) formalize memorization as the ability of a model to correctly predict a label only
 077 if the sample was present in the training data. Their analysis suggests that the key obstacle to
 078 generalization is not label noise but suboptimal sampling, with many regions of the data distribution
 079 undersampled or represented by only a single example. We compare our proposed memorization
 080 metric in detail to the work of Feldman & Zhang (2020) in Appendix A.12. Even though these
 081 atypical examples in so-called long-tailed data distributions are memorized individually to reach
 082 high training performance, this memorization leads to improved generalization of the network (cf.
 083 Feldman & Zhang (2020)).

084 Building on this perspective, Baldock et al. (2021) observe that deep models first capture simple
 085 patterns shared across many examples, before gradually fitting more complex patterns that may be
 086 unique to a small subset of the data or even example-specific. A similar observation can be found in
 087 Liu et al. (2020), where the authors develop a framework to leverage that property to be able to learn
 088 in noisy scenarios. Bayat et al. (2024) argue that memorization is not inherently detrimental, but
 089 rather depends on factors such as data quality and learning dynamics. They introduce the notion of
 090 an example-specific feature rate, showing that excessively high rates prevent models from capturing
 091 the underlying distribution, while excessively low rates encourage the learning of overly complex
 092 representations, leading to catastrophic overfitting.

093 Subsequent work examined memorization, including studies by Carlini et al. (2019) and Yun et al.
 094 (2019), with particular attention to the effects of heavy overparameterization (Zhang et al., 2020)
 095 and minimal overparameterization (Daniely, 2020). Another line of research examines where memo-
 096 rization occurs within a network. For instance, Maini et al. (2023) demonstrate that memorization
 097 is localized across layers and even within specific neurons. Our approach is closely aligned with
 098 this perspective: by attaching RLP-heads at different layers, we obtain a direct means of localizing
 099 memorization.

100 Memorization effects are particularly pronounced in large-scale language models, where they raise
 101 significant privacy concerns if training data can be extracted from the models, as highlighted by
 102 Tirumala et al. (2022) and Carlini et al. (2021). Efforts to improve generalization and mitigate data
 103 memorization have largely focused on general-purpose regularization methods, such as dropout
 104 (Srivastava et al., 2014) and weight decay (Krogh & Hertz, 1991). However, to the best of our
 105 knowledge, no existing approach explicitly regularizes memorization itself, as we propose in this
 106 work.

107 Close related challenges arise in the context of fair AI, where suppression of unwanted or spurious
 108 features is critical to prevent models from encoding biases related to attributes such as gender, ethnic-
 109 ity, or religion (Mehrabi et al., 2021; Tian et al., 2022; Wang et al., 2020; Zhang et al., 2018a). We
 110 take technical inspiration from this field to develop our memorization suppressing regularizer. Finally,
 111 our interpretation of random label accuracy as a proxy for information abstraction bears conceptual

108 resemblance to mutual information frameworks, which have been applied to analyze ANNs (Gabrié
 109 et al., 2018).
 110

111 3 BACKGROUND: RADEMACHER COMPLEXITY

112 We take inspiration from the Rademacher complexity measure to motivate our empirical metric.
 113 Rademacher complexity is a fundamental tool in statistical learning theory, quantifying the expressive
 114 power of a model (or hypothesis class) by measuring its ability to fit random labels. In the case of
 115 binary classification, it can be defined as follows:

116 **(Empirical) Rademacher complexity for Binary Classification (Mohri et al., 2012):** Given a
 117 hypothesis class \mathcal{H} and train data $\mathcal{S} = \{(x_1, \sigma_1), \dots, (x_m, \sigma_m)\}$, where $\sigma_1, \dots, \sigma_m \in \{\pm 1\}$ are i.i.d.
 118 uniform random variables:

$$119 \hat{\mathfrak{R}}_{\mathcal{S}}(\mathcal{H}) = \mathbb{E}_{\sigma} \left[\sup_{h \in \mathcal{H}} \frac{1}{m} \sum_{i=1}^m \sigma_i h(x_i) \right] \quad (1)$$

120 In binary classification, the agreement between a model’s prediction and the true label can be quantified
 121 by the product of the label and the model output. While this measure is closely related to
 122 accuracy, it is inherently restricted to the binary setting and does not naturally extend to multi-class
 123 classification. The hypothesis h is chosen as a supremum over the hypothesis class, which in practice
 124 can be approximated via empirical risk minimization (e.g., with optimizers such as SGD or Adam).
 125 However, the presence of the supremum makes the exact evaluation of Rademacher complexity
 126 intractable in practical settings.

127 Importantly, it is model-agnostic, and therefore explicitly independent of architectural details including
 128 depth, width, and the total number of parameters. Instead, it captures the capacity of a model
 129 through its ability to fit random labels. Within the PAC-learning framework, this quantity is central to
 130 deriving bounds on the generalization error. In particular, for binary classification, the generalization
 131 error can be bounded as:

132 *Theorem 1.* Given a hypothesis class \mathcal{H} , training data $\mathcal{S} = \{(x_1, \sigma_1), \dots, (x_m, \sigma_m)\}$, with
 133 $\sigma_1, \dots, \sigma_m \in \{\pm 1\}$, then for any $\delta > 0$, with probability at least $1 - \delta$ for any $h \in \mathcal{H}$ it holds
 134 that

$$135 R(h) \leq \hat{R}_{\mathcal{S}}(h) + \hat{\mathfrak{R}}_{\mathcal{S}}(\mathcal{H}) + 3\sqrt{\frac{\log(2/\delta)}{2m}}.$$

136 Where $\hat{R}_{\mathcal{S}}(h)$ denotes the empirical error on the training dataset (Mohri et al., 2012). This bound
 137 implies that, for fixed training performance, a reduction in Rademacher complexity directly translates
 138 into improved test performance bounds and thus tightens limits on the generalization error. While
 139 Rademacher complexity provides a theoretically powerful framework for characterizing the capacity
 140 of hypothesis classes, its exact computation for state-of-the-art deep learning models is infeasible.
 141 Inspired by this theoretical foundation, we will derive an empirical alternative to Rademacher
 142 complexity, suited for real-world training tasks, thereby enabling the study of the relation between
 143 memorization and generalization in practical deep learning settings.

144 4 RANDOM LABEL PREDICTIONS AND REGULARIZATION

145 Rather than training an entire network on random labels, as explored in prior work, we introduce
 146 an auxiliary Random Label Prediction Head (RLP-head) that predicts a randomly assigned label
 147 in parallel with the standard classification task. Concretely, the proposed architecture outputs both
 148 the task prediction vector $p \in \mathbb{R}^N$ and an additional random label prediction vector $\hat{p} \in \mathbb{R}^n$. While
 149 the number of task classes N is determined by the dataset, the number of possible random labels n
 150 can be chosen arbitrarily. The RLP-head may be attached at different locations within the network.
 151 Unless otherwise specified, we place it after the penultimate layer, in parallel with the standard
 152 classification head. This choice is natural since the penultimate activations correspond to the final
 153 stage of the feature extractor, and the RLP-head thereby probes the extent of memorization within the
 154 learned final representation.

155 Random labels are generated once at the beginning of the training and remain fixed across epochs for
 156 each sample. Only the RLP-head receives gradients from the random label objective, ensuring that
 157 the normal classification head is unaffected. Consequently, our method enables probing memorization

162 without affecting normal task performance.
163

164 In order to train the RLP-head we introduce
165 an auxiliary cross-entropy loss on the random
166 labels, L^{rnd} , in addition to the standard classifi-
167 cation loss, L^{class} , where y denotes the correct
168 class label and \hat{y} the assigned random label:

$$169 \quad L^{class} = - \sum_{i=1}^N \delta_{iy} \log(p_i) = - \log(p_y) \quad (2)$$

$$173 \quad L^{rnd} = - \sum_{i=1}^n \delta_{i\hat{y}} \log(\hat{p}_i) = - \log(\hat{p}_{\hat{y}}) \quad (3)$$

175 By default, we implement the RLP-head as a
176 single fully-connected layer followed by a soft-
177 max activation. Nevertheless, the architecture
178 of the RLP-head is flexible, and more complex
179 variants can be used (see Appendix A.6 for re-
180 sults with a two-layer head).

181 Training the RLP-head on random labels in par-
182 allel with the main task enables to directly regu-
183 larize memorization during standard training. Since we interpret the accuracy of the random label
184 predictions provides a means of constraining the effective complexity of the model.
185 Therefore, we introduce a regularization loss term that penalizes correct predictions of the random
186 labels by the RLP-head. Specifically, this loss is derived from the standard cross-entropy formulation:

$$188 \quad L^{reg} = \sum_{i=1}^n \delta_{i\hat{y}} \log(1 - \hat{p}_i) = \log(1 - \hat{p}_{\hat{y}}). \quad (4)$$

191 Compared with standard cross-entropy, we invert the sign of the loss, since the regularizer is designed
192 to prevent the network from learning the random labels. Furthermore, we replace \hat{p}_i with $1 - \hat{p}_i$
193 inside the logarithm, which amplifies the penalty when $\hat{p}_i \approx 1$. This ensures that highly confident
194 predictions of random labels are penalized more strongly. The resulting regularization term is scaled
195 by a tunable hyperparameter λ and added to the loss of the feature extractor.

196 Although the regularization loss is computed using the RLP-head, its gradients are restricted to the
197 feature extractor. Accordingly, the classification head remains unaffected during RLP-regularization.
198 A schematic of the proposed architecture is provided in Figure 1. Conceptually, the RLP-head and
199 the feature extractor form two adversarial components: the RLP-head attempts to fit the random
200 labels, while the feature extractor is regularized to prevent this from happening. This adversarial
201 setup encourages the feature extractor to produce representations that are less example-specific and
202 do not allow memorization of specific inputs. The proposed regularizer is, therefore, used here as a
203 tool to investigate the effects of memorization in different parts of the network.

204 5 EXPERIMENTS

206 Details of our experimental setup can be found in Appendix A.1.
207

208 5.1 LEARNING RANDOM LABELS

210 Throughout this section, we analyze the training of the RLP-head, such that it serves solely as a
211 metric and does not influence network performance (i.e., $\lambda = 0$). Figure 2A shows the test and train
212 accuracy of the classification head alongside the random label accuracy extracted from the RLP-head
213 for ViT-B/32 trained on ImageNet. Around epoch 20, test and train accuracies begin to diverge,
214 indicating the beginning of overfitting. Notably, the random label accuracy starts to rise slightly
215 earlier, reaching approximately 70 % by the end of training. This shows that, even when trained
exclusively on correct class labels, the model memorizes a substantial portion of the dataset enough

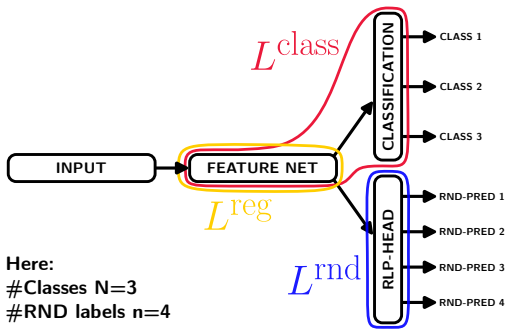
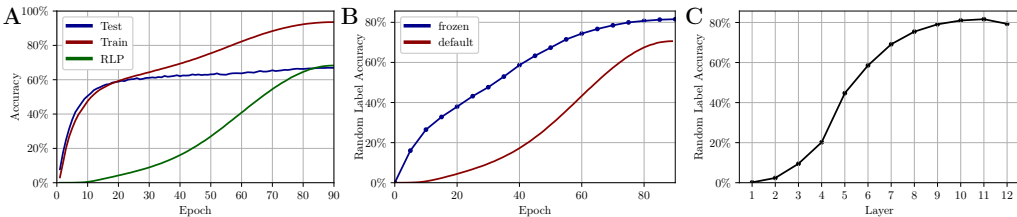


Figure 1: An additional Random Label Prediction Head (RLP-head) is added after the feature extractor of the network. Only the RLP-head receives L^{rnd} , the random label prediction loss, whereas the regularizing loss L^{reg} is calculated on the RLP-head but acts on the feature extractor only.

216 for a single fully-connected layer to correctly predict random labels. The fact that random label
 217 accuracy does not approach 100 % may reflect that the chosen network architecture does not have
 218 sufficient capacity to fully memorize the dataset, consistent with the training accuracy plateauing at
 219 roughly 93 %.

220 Since we train the RLP-head together with the main classifier, we cannot tell whether its low
 221 early-epoch accuracy is due to the RLP-head not having been trained long enough or because the
 222 network has not yet memorized many samples. To disentangle these effects, we performed an
 223



224 Figure 2: ViT-B/32 on ImageNet. **A:** The proposed single fully-connected layer as RLP-head is
 225 sufficient to correctly predict approx. 70 % of the random labels, indicating that the feature extractor
 226 memorizes a substantial portion of the training set. **B:** Even after freezing the feature extractor,
 227 RLP-head attains low accuracy in the early epochs, confirming that the default RLP-head approach
 228 reliably tracks the evolution of memorization dynamics during training. **C:** Random label accuracy
 229 when attaching the RLP-head at various network depths. The higher accuracy observed in deeper
 230 layers indicates that increasingly abstract representations still retain sample-specific information
 231 allowing for memorization.

232 additional experiment with two different modes of training the RLP-head shown in Figure 2B. *Default*
 233 refers to training the RLP-head in parallel with the main task, as described previously. *Frozen* refers
 234 to freezing all layers except the RLP-head at checkpoints saved after each epoch, and subsequently
 235 training (only) the RLP-head *from scratch*. For all frozen runs, the RLP-head is initialized with the
 236 same parameters and trained on the same fixed set of random labels. This setup ensures that the
 237 RLP-head receives sufficient and equal training capacity at each epoch. At epoch 0 (random weights),
 238 the frozen training fails to fit the random labels, indicating that the signal measured by the default
 239 training actually stems from memorization learned by the feature extractor during training and not
 240 from limitations of the RLP-head. Although this frozen training does not allow for regularization
 241 and is computationally very demanding, it is shown here to validate the suitability of our proposed
 242 default training method.

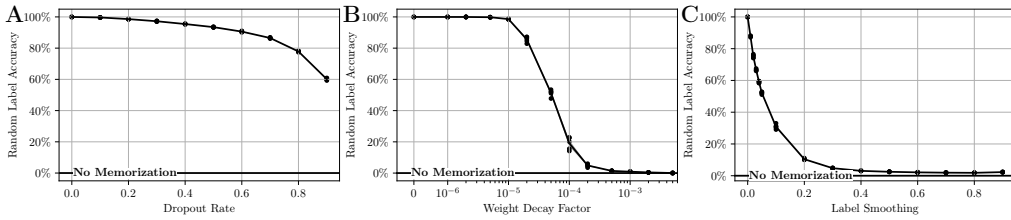
243 We further investigate where memorization occurs within the network by attaching a separate
 244 RLP-head consisting of a normalization layer, a fully-connected layer and a softmax layer after
 245 each transformer block of a ViT-B/32 trained on ImageNet (Figure 2C). The random label accuracy
 246 increases with the network depth: After the first layer nearly 0 % of the random labels can be predicted
 247 correctly, while high accuracies are reached in later layers. Similar to the previous experiment, this
 248 dependency shows that the RLP-head does not itself memorize the input sample but instead reflects
 249 the representational properties of the network. After the first layer, where only minimal processing
 250 occurred, the activations retain a significant amount of sample-specific information. Interestingly,
 251 this does not lead to an increased random label accuracy. Instead, high random label accuracies are
 252 reached only after sufficient abstraction of the features, showing that the abstracted features are still
 253 sample-specific and lead to memorization.

254 5.2 RELATION TO OTHER COMPLEXITY REGULARIZERS

255 We propose to use the accuracy of the RLP-head as a proxy for model complexity, providing an
 256 empirical approximation to Rademacher complexity. To validate this interpretation, we evaluate our
 257 metric under three well-established regularization strategies, namely dropout, weight decay, and label
 258 smoothing. As illustrated in Figure 3, each of these regularizers consistently suppresses random label
 259 accuracy, confirming the correlation of the random label accuracy with model complexity.

260 We further support this correlation by studying the impact of the model size on the random label
 261 accuracy in Appendix A.9. We also use the random label accuracy to demonstrate that mixup reduces -
 262 but does not fully eliminate - memorization in Appendix A.16. Additional experiments with ViT-S/32

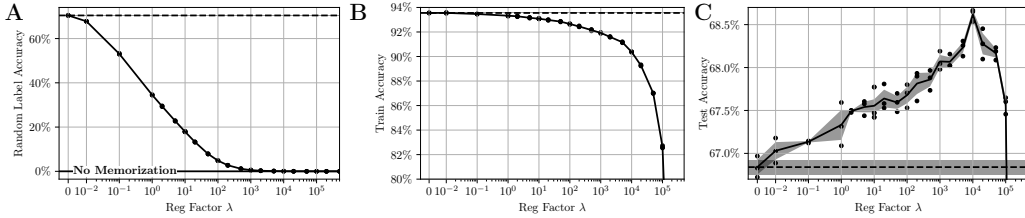
270 on ImageNet comparing the proposed random label accuracy against measuring memorization via
 271 noisy labels for different regularizers can be found in Appendix A.14.
 272



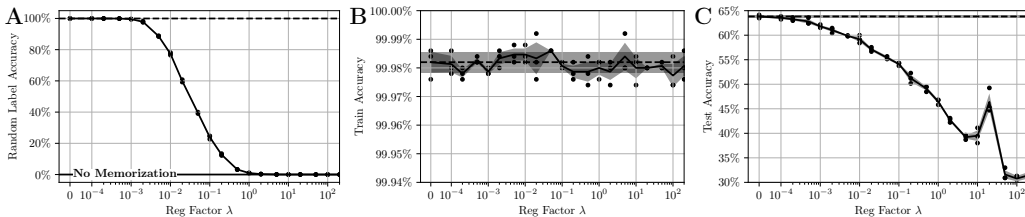
280 Figure 3: WRN16-4 on CIFAR-100. The effect of common complexity regularizers can be measured
 281 with the proposed metric. **A:** Dropout. **B:** Weight decay. **C:** Label smoothing.
 282

283 284 285 5.3 REGULARIZING RANDOM LABELS

286 We can use the RLP-head to explicitly regularize the memorization of the network. To accomplish
 287 this, we apply the loss term defined in Equation 4 and search for an optimal regularization factor λ .
 288 We report results for ViT-B/32 on ImageNet in Figure 4 and WideResNet-16-4 on CIFAR-100 in
 289 Figure 5. We find that RLP-regularization effectively suppresses memorization in both experimental
 290



291 Figure 4: ViT-B/32 on ImageNet. Random label, train and test accuracy under RLP-regularization for
 292 different regularization factors λ . RLP-regularization effectively reduces memorization, and leads to
 293 better generalization (smaller test-train gap) and test performance.
 294



301 Figure 5: WideResNet-16-4 on CIFAR-100. Random label, train and test accuracy under RLP-
 302 regularization for different regularization factors λ . Here, RLP-regularization effectively reduces
 303 memorization, but does not improve generalization.
 304

314 settings reducing the random label accuracy down to the level expected from random guessing.
 315 On ImageNet with ViT, this effect translates into improved generalization: while training accuracy
 316 decreases, test accuracy increases, reaching a peak of 68.5 % at $\lambda = 10^4$, which corresponds to a gain
 317 of 1.5 % over the baseline. The simultaneous drop in training accuracy further narrows the train–test
 318 gap, confirming the effectiveness of RLP-regularization to reduce overfitting. These observations
 319 align with predictions from PAC-learning theory based on Rademacher complexity, as well as the
 320 intuition that memorization causes overfitting and harms generalization.

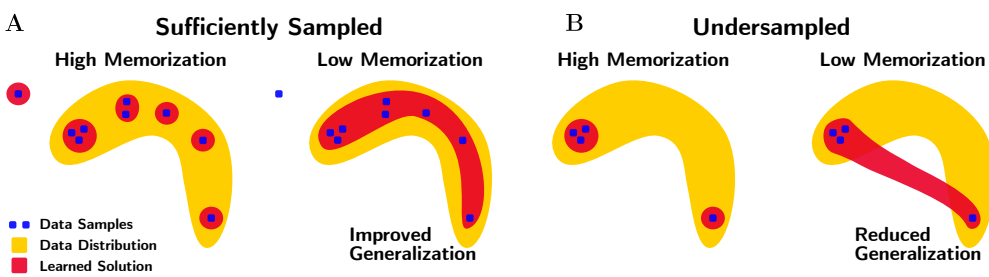
321 Interestingly, these findings do not hold for our experiments for WideResNet-16-4 on CIFAR-100.
 322 Instead, the training accuracy remains unaffected, while the test accuracy deteriorates even for small
 323 regularization factors. These deviations from classical theory are consistent with recent findings,
 e.g., by (Nakkiran et al., 2021), which highlight the distinct dynamics of modern overparameterized

324 networks. Our results suggest that the relationship between memorization and generalization is more
 325 nuanced than traditional theory predicts, which we study further in the following sections.
 326

327 5.4 UNDERSAMPLED DATASETS BENEFIT FROM MEMORIZATION 328

329 Based on our findings and drawing on insights from Feldman (2019) and Bayat et al. (2024), we
 330 hypothesize two distinct memorization scenarios that reconcile the apparent contradictions with the
 331 classical view of overfitting.

332 Memorization corresponds to the adoption of features that are highly specific to individual samples.
 333 Suppressing memorization prevents the learning of sample-specific features, forcing it instead to focus
 334 on features shared across examples of the same class. When sufficient samples are available, this
 335 results in learning features of the underlying true data distribution leading to increased generalization
 336 (cf. Figure 6A). Without memorization, training accuracy decreases because the network may fail to
 337 fit atypical samples, especially those that share few features with other samples in the same class, such
 338 as noisy or mislabeled samples. We hypothesize that this mechanism explains the observed behavior
 339 on ImageNet (Figure 4). However, when the dataset is undersampled and memorization is suppressed,
 340



341 Figure 6: Schematic illustration of how memorization can be either detrimental or benign depending
 342 on dataset sampling. Under memorization, the model learns sample-specific solutions (depicted as
 343 small isolated regions around individual samples). In contrast, suppressing memorization encourages
 344 the discovery of a single connected solution space that better captures class-level structure while
 345 excluding outliers such as noisy or mislabeled samples.
 346

347 the shared features learned across class samples may fail to reflect the true data distribution and
 348 instead capture arbitrary artifacts of the insufficient sampling. In this case, suppressing memorization
 349 forces the network to rely on these spurious shared features, which degrades generalization. New,
 350 unseen samples may still resemble individual memorized training examples but are unlikely to share
 351 the learned spurious features shared by training examples from undersampled regions of the true data
 352 distribution (cf. Figure 6B). We hypothesize that this mechanism explains the behavior observed
 353 on CIFAR-100 (Figure 5). In line with this view, we find the same effect (reduced random label
 354 accuracy, stable training accuracy, and degraded test accuracy) when applying the RLP-regularizer to
 355 ViT trained on CIFAR-100 (Appendix A.3).

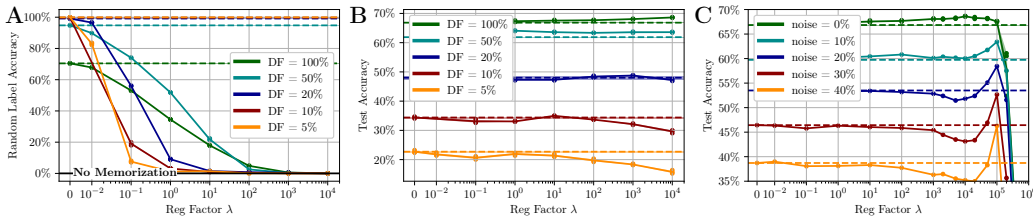
356 To further test this hypothesis, we study the impact of dataset size by training ViT-B/32 on subsets of
 357 ImageNet while keeping the experimental setup fixed. As shown in Figure 7, our regularizer improves
 358 test accuracy only when large fractions of the dataset are available. The conventional intuition that
 359 memorization is always detrimental would suggest that reducing memorization should be even more
 360 beneficial on smaller datasets, where higher memorization (as observed by higher random label
 361 accuracy) occurs. Our experiment thus provides evidence in support of our hypothesis of beneficial
 362 memorization effects for undersampled datasets.

363 We perform an additional experiment where we inject label noise into the training dataset and apply
 364 the RLP-regularizer. Since noisy labels cannot contribute positively to generalization and can only be
 365 fit through memorization, our regularizer should consistently improve test performance in this setting.
 366 This prediction is confirmed in Figure 7C.

367 Related findings were also reported by Feldman (2019), who argue that memorization in sparsely
 368 sampled regions of the data distribution (i.e., the long tail) can actually enhance generalization.
 369 Because the proposed RLP-regularizer directly suppresses memorization, we apply it to the ImageNet-
 370 LT dataset (Liu et al., 2019b) to demonstrate in Appendix A.19 that classes in the long tail (i.e., those
 371 with few training samples) can no longer be predicted correctly when memorization is inhibited.

372 Taken together, our experiments highlight both detrimental and beneficial aspects of memorization
 373

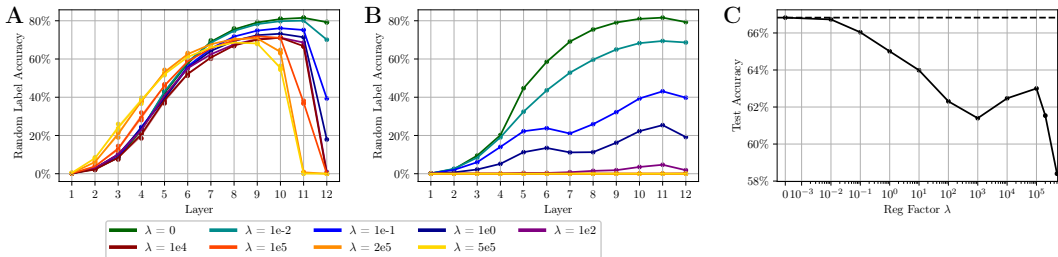
378 and demonstrate that RLP-heads, along with the derived regularizer, provide an effective framework
 379 for probing and controlling these dynamics.
 380



381
 382 Figure 7: ViT-B/32 on ImageNet. **A+B:** Random label and test accuracy when training on reduced
 383 dataset fractions (DF) of ImageNet. Although smaller training sets lead to stronger memorization
 384 (higher random label accuracy), suppressing memorization on them does not improve test accuracy.
 385 **C:** Test accuracy with added label noise under RLP-regularization. Since memorization of noisy
 386 labels hinders generalization, our regularizer yields substantial improvements.
 387

388 5.5 RLP-REGULARIZATION SHIFTS MEMORIZATION

389 To further understand the effects of the RLP-regularizer, we analyze memorization across different
 390 layers of the network. We attach additional RLP-heads after each layer of a vision transformer, as
 391 described above. Figure 8A shows the resulting random label accuracy across layers for varying
 392 regularization strengths.
 393



401
 402 Figure 8: ViT-B/32 on ImageNet. **A:** Random label accuracy of RLP-heads at different layers when
 403 only the final (12th) layer is used for RLP-regularization. Memorization shifts toward earlier layers.
 404 **B+C:** RLP-regularization is calculated based on RLP-heads attached to all 12 transformer layers.
 405 While this effectively suppresses memorization and prevents the shift, neither test accuracy nor
 406 generalization improve.
 407

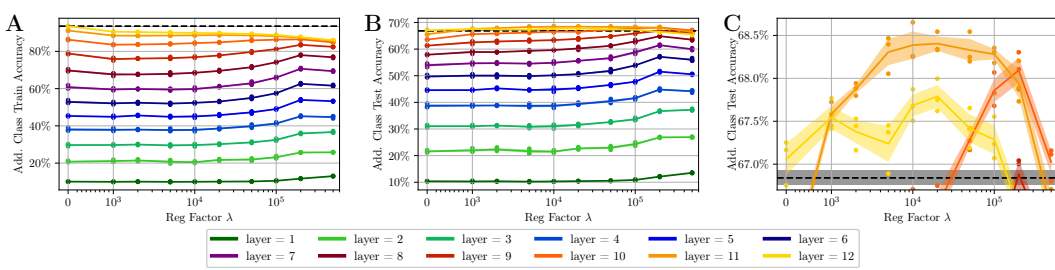
408 The RLP-regularization is only applied based on the RLP-head attached to the final (12th) layer.
 409 Consequently, the random label accuracy drops rapidly for this last layer with increasing regularization.
 410 RLP-heads near the regularized final layer, particularly layers 10 and 11, are also affected. In contrast,
 411 earlier layers exhibit the opposite effect: RLP-heads attached to layers 2 to 6 achieve higher random
 412 label accuracies under regularization. This indicates that while memorization is mitigated in the last
 413 layer, it is shifted to earlier layers rather than eliminated. We hypothesize that, in response to the
 414 RLP-regularizer, the network transforms sample-specific features into class-relevant information in
 415 earlier layers, thereby enabling memorization to persist while being undetected by the regularizing
 416 RLP-head attached to the final layer.

417 To test this hypothesis, we conduct an additional experiment, adding a classification head to each
 418 transformer layer trained to predict the class label. This setup enables tracking the transformation
 419 from sample-specific features to class information throughout the network. Figure 9 shows the
 420 resulting class, train, and test accuracies under RLP-regularization based on the final layer. While
 421 class accuracy decreases in the last layer and the penultimate layer (11), we observe increased
 422 accuracy in earlier layers for both training and test data. Remarkably, test accuracies at layers 10
 423 and 11 even surpass those of layer 12 (Figure 9C), indicating that regularization not only shifts
 424 memorization and classification capabilities but can also improve generalization in earlier layers.
 425

432 This supports the hypothesis that RLP-regularization shifts the transformation into class-specific
 433 information to earlier layers.

434 Next, we examine the effect of suppressing memorization when using all attached RLP-heads for our
 435 regularization. As shown in Figure 8B, this effectively reduces random label accuracy at all layers,
 436 even for modest regularization strengths. However, this does not translate into improved test accuracy
 437 (Figure 8C). We hypothesize that applying RLP-regularization to all layers constitutes an overly harsh
 438 intervention: Extraction of sample-specific features in early layers may be useful even when these
 439 features do not lead to direct memorization. Moreover, some degree of memorization may persist
 440 within a transformer block itself, being hidden to the respective RLP-head attached at its end. We
 441 further study this hypothesis in Appendix A.20.

442 Additionally, we study the influence of the regularizer when the loss term is constructed from a single
 443 RLP-head attached to an intermediate layer in Appendix A.10.



444
 445
 446
 447
 448
 449
 450
 451
 452
 453 Figure 9: ViT-B/32 on ImageNet. Similar to the RLP-heads, we attach additional classification heads
 454 to the outputs of all layers in a ViT to track the transformation from sample-specific features to class
 455 predictions throughout the network. When applying RLP-regularization to the final (12th) layer only,
 456 class prediction accuracy increases in the earlier layers and test performance improves across all
 457 layers. **A:** Train accuracy. **B:** Test accuracy. **C:** Zoomed-in view of test accuracy.

460 6 CONCLUSION

461 We have introduced an effective method to measure and regularize memorization in deep neural
 462 networks: random layer prediction heads (RLP-heads), which can be attached to any (intermediate)
 463 network activation. Motivated as an empirical approximation of Rademacher complexity, we demon-
 464 strated that random label accuracy serves as a valid metric for network complexity and memorization.
 465 This metric enables the study of both the temporal (i.e., during optimization) and spatial (i.e., across
 466 layers) dynamics of memorization within a network. Based on the RLP-heads, we derived a regular-
 467 ization method to explicitly mitigate learning of sample-specific features and in consequence stop
 468 memorization.

469 Our experiments show that memorization can be either beneficial or detrimental for generalization
 470 deep neural networks. We propose a hypothesis to explain this counterintuitive effect based on dataset
 471 sampling and support it with targeted experiments. Moreover, applying the memorization regularizer
 472 to the final layer shifts both abstraction of class-level representations and memorization into earlier
 473 layers, resulting in a network that achieves better generalization after fewer layers.

474 Our findings highlight the value of RLP-heads and RLP-regularization for studying memorization
 475 and suggest their broader potential for empirical analysis of deep learning mechanisms.

486 REPRODUCIBILITY STATEMENT
487488 For all experiments, we report complete results, including the outcomes of all hyperparameter
489 searches. Details on training configurations are provided in Appendix A.1. The source code is
490 included in the supplementary material and will be released publicly upon acceptance.
491492 LLM USAGE
493494 Large language models (LLMs) were used exclusively to assist in refining the phrasing of certain
495 sentences and improving the clarity of formulations in this manuscript. At no point were LLMs
496 employed for data analysis, generation of scientific content, or drawing conclusions. All scientific
497 claims, results, and interpretations are the sole work of the authors.
498499 REFERENCES
500

501 Devansh Arpit, Stanisław Jastrzebski, Nicolas Ballas, David Krueger, Emmanuel Bengio, Maxinder S.
502 Kanwal, Tegan Maharaj, Asja Fischer, Aaron Courville, Yoshua Bengio, and Simon Lacoste-Julien.
503 A Closer Look at Memorization in Deep Networks. *International Conference on Machine Learning*,
504 2017.

505 Robert J. N. Baldock, Hartmut Maennel, and Behnam Neyshabur. Deep learning through the lens of
506 example difficulty. *Advances in Neural Information Processing Systems*, 2021.

507 Björn Barz and Joachim Denzler. Do we train on test data? purging cifar of near-duplicates. *Journal
508 of Imaging*, 6(6), 2020.

509 Reza Bayat, Mohammad Pezeshki, Elvis Dohmatob, David Lopez-Paz, and Pascal Vincent. The
510 pitfalls of memorization: When memorization hurts generalization. *arXiv:2412.07684 [cs]*, 2024.

511 Nicholas Carlini, Chang Liu, Úlfar Erlingsson, Jernej Kos, and Dawn Song. The secret sharer:
512 evaluating and testing unintended memorization in neural networks. In *USENIX Conference on
513 Security Symposium*, pp. 267–284, 2019.

514 Nicholas Carlini, Florian Tramèr, Eric Wallace, Matthew Jagielski, Ariel Herbert-Voss, Katherine
515 Lee, Adam Roberts, Tom Brown, Dawn Song, Úlfar Erlingsson, Alina Oprea, and Colin Raffel. Ex-
516 tracting training data from large language models. In *USENIX Conference on Security Symposium*,
517 pp. 2633–2650, 2021.

518 Francesco Croce and Matthias Hein. Reliable evaluation of adversarial robustness with an ensemble
519 of diverse parameter-free attacks. In *Proceedings of the 37th International Conference on Machine
520 Learning*, 2020.

521 Amit Daniely. Neural networks learning and memorization with (almost) no over-parameterization.
522 *Advances in Neural Information Processing Systems*, 2020.

523 Jia Deng, Wei Dong, Richard Socher, Li-Jia Li, Kai Li, and Li Fei-Fei. Imagenet: A large-scale
524 hierarchical image database. *Conference on Computer Vision and Pattern Recognition*, 2009.

525 Alexey Dosovitskiy, Lucas Beyer, Alexander Kolesnikov, Dirk Weissenborn, Xiaohua Zhai, Thomas
526 Unterthiner, Mostafa Dehghani, Matthias Minderer, Georg Heigold, Sylvain Gelly, Jakob Uszkoreit,
527 and Neil Houlsby. An image is worth 16x16 words: Transformers for image recognition at scale.
528 *International Conference on Learning Representations*, 2021.

529 Vitaly Feldman. Does learning require memorization? A short tale about a long tail. In *Proceedings
530 of the 52nd Annual ACM SIGACT Symposium on Theory of Computing*, volume abs/1906.05271,
531 2019.

532 Vitaly Feldman and Chiyuan Zhang. What neural networks memorize and why: Discovering the long
533 tail via influence estimation. *Advances in Neural Information Processing Systems*, 2020.

540 Marylou Gabrié, Andre Manoel, Clément Luneau, Jean Barbier, Nicolas Macris, Florent Krzakala,
 541 and Lenka Zdeborová. Entropy and mutual information in models of deep neural networks.
 542 *Advances in Neural Information Processing Systems*, 2018.

543

544 Ian J. Goodfellow, Jonathon Shlens, and Christian Szegedy. Explaining and harnessing adversarial
 545 examples. In *International Conference on Learning Representations*, 2018.

546

547 Alex Krizhevsky and Geoffrey Hinton. Learning multiple layers of features from tiny images.
 548 Technical report, University of Toronto, 2009.

549

550 Anders Krogh and John Hertz. A simple weight decay can improve generalization. *Advances in
 551 Neural Information Processing Systems*, 1991.

552

553 Sheng Liu, Jonathan Niles-Weed, Narges Razavian, and Carlos Fernandez-Granda. Early-learning
 554 regularization prevents memorization of noisy labels. *Advances in Neural Information Processing
 555 Systems*, 2020.

556

557 Yinhan Liu, Myle Ott, Naman Goyal, Jingfei Du, Mandar Joshi, Danqi Chen, Omer Levy, Mike
 558 Lewis, Luke Zettlemoyer, and Veselin Stoyanov. Roberta: A robustly optimized BERT pretraining
 559 approach. *arXiv:1907.11692 [cs]*, 2019a.

560

561 Ziwei Liu, Zhongqi Miao, Xiaohang Zhan, Jiayun Wang, Boqing Gong, and Stella X Yu. Large-scale
 562 long-tailed recognition in an open world. In *Proceedings of the IEEE/CVF conference on computer
 563 vision and pattern recognition*, 2019b.

564

565 Ilya Loshchilov and Frank Hutter. Decoupled weight decay regularization. *International Conference
 566 on Learning Representations*, 2019.

567

568 Aleksander Madry, Aleksandar Makelov, Ludwig Schmidt, Dimitris Tsipras, and Adrian Vladu.
 569 Towards deep learning models resistant to adversarial attacks. In *International Conference on
 570 Learning Representations*, 2018.

571

572 Pratyush Maini, Michael C. Mozer, Hanie Sedghi, Zachary C. Lipton, J. Zico Kolter, and Chiyuan
 573 Zhang. Can neural network memorization be localized? *International Conference on Machine
 574 Learning*, 2023.

575

576 Ninareh Mehrabi, Fred Morstatter, Nripsuta Saxena, Kristina Lerman, and Aram Galstyan. A survey
 577 on bias and fairness in machine learning. *ACM Comput. Surv.*, 54(6):35, 2021.

578

579 Mehryar Mohri, Afshin Rostamizadeh, and Ameet Talwalkar. *Foundations of machine learning*.
 580 Adaptive Computation and Machine Learning series. MIT Press, 2012.

581

582 Preetum Nakkiran, Gal Kaplun, Yamini Bansal, Tristan Yang, Boaz Barak, and Ilya Sutskever. Deep
 583 double descent: Where bigger models and more data hurt. *Journal of Statistical Mechanics: Theory
 584 and Experiment*, 2021(12):124003, 2021.

585

586 Nitish Srivastava, Geoffrey Hinton, Alex Krizhevsky, Ilya Sutskever, and Ruslan Salakhutdinov.
 587 Dropout: A simple way to prevent neural networks from overfitting. *Journal of Machine Learning
 588 Research*, 15(56):1929–1958, 2014.

589

590 Huan Tian, Tianqing Zhu, Wei Liu, and Wanlei Zhou. Image fairness in deep learning: problems,
 591 models, and challenges. *Neural Computing and Applications*, 34:12875–12893, 2022.

592

593 Kushal Tirumala, Aram Markosyan, Luke Zettlemoyer, and Armen Aghajanyan. Memorization
 594 without overfitting: Analyzing the training dynamics of large language models. *Advances in Neural
 595 Information Processing Systems*, 2022.

596

597 Zeyu Wang, Clint Qinami, Ioannis Christos Karakozis, Kyle Genova, Prem Nair, Kenji Hata, and Olga
 598 Russakovsky. Towards Fairness in Visual Recognition: Effective Strategies for Bias Mitigation. In
 599 *Conference on Computer Vision and Pattern Recognition*, 2020.

600

601 Chulhee Yun, Suvrit Sra, and Ali Jadbabaie. Small relu networks are powerful memorizers: a tight
 602 analysis of memorization capacity. *Advances in Neural Information Processing Systems*, 2019.

594 Sergey Zagoruyko and Nikos Komodakis. Wide residual networks. *British Machine Vision Conference*, 2016.
595
596

597 Brian Hu Zhang, Blake Lemoine, and Margaret Mitchell. Mitigating unwanted biases with adversarial
598 learning. In *Proceedings of the 2018 AAAI/ACM Conference on AI, Ethics, and Society*, pp.
599 335–340. ACM, 2018a.

600 Chiyuan Zhang, Samy Bengio, Moritz Hardt, Michael C. Mozer, and Yoram Singer. Identity crisis:
601 Memorization and generalization under extreme overparameterization. *International Conference
602 on Learning Representations*, 2020.

603 Chiyuan Zhang, Samy Bengio, Moritz Hardt, Benjamin Recht, and Oriol Vinyals. Understanding
604 deep learning (still) requires rethinking generalization. *Commun. ACM*, 64(3):107–115, 2021.

605 Hongyi Zhang, Moustapha Cisse, Yann N. Dauphin, and David Lopez-Paz. mixup: Beyond empirical
606 risk minimization. In *International Conference on Learning Representations*, 2018b.

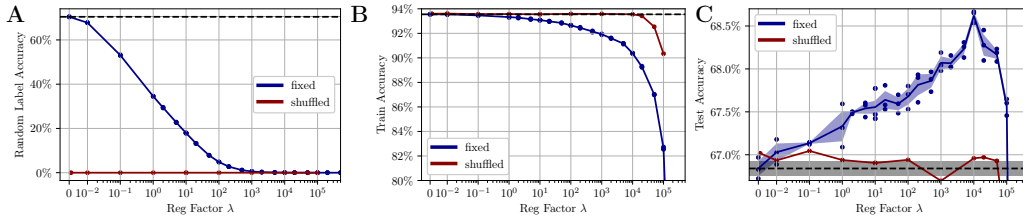
607 Xiang Zhang and Yann LeCun. Text understanding from scratch. *arXiv:1502.01710 [cs]*, 2016.

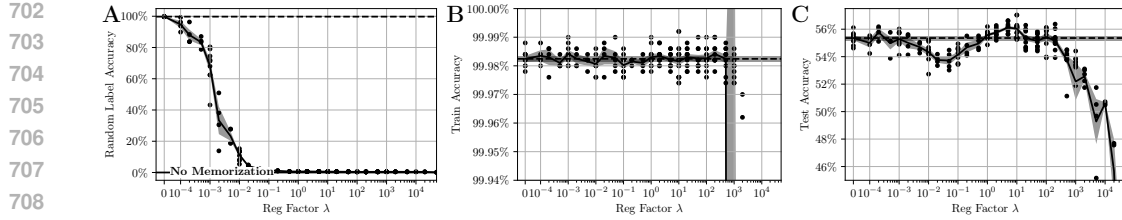
608
609
610
611
612
613
614
615
616
617
618
619
620
621
622
623
624
625
626
627
628
629
630
631
632
633
634
635
636
637
638
639
640
641
642
643
644
645
646
647

648 APPENDIX
649650 A.1 EXPERIMENTAL SETUP
651652 In the main text we focus on two evaluation scenarios:
653

654

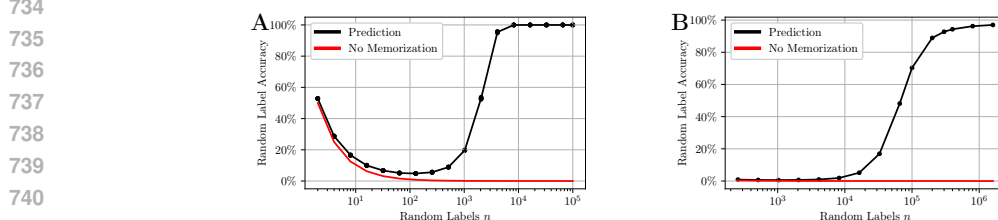
- 655 1. WideResNet-16-4 (Zagoruyko & Komodakis, 2016) on CIFAR-100 (Krizhevsky & Hinton, 656 2009) trained with SGD with momentum $\mu = 0.9$, a linear learning rate warm up in the first 657 epoch followed by a cosine decay with base learning rate of $\eta = 0.5$ and a batch size of 658 256 trained for 200 epochs without additional regularization or data augmentation. We use 659 $n = 10,000$ as the number of (different) random labels.
660
- 661 2. ViT-B/32 (Dosovitskiy et al., 2021) on ImageNet-1k (Deng et al., 2009) trained with AdamW 662 (Loshchilov & Hutter, 2019) and learning rate warm up for eight epochs followed by a 663 cosine decay with base learning rate of $\eta = 0.001$ and a batch size of 1024 trained for 90 664 epochs with flipping augmentation, gradient clipping ($\ell_{max}^2 = 1.0$) and weight decay of 0.1. We 665 use $n = 100,000$ random labels.
666

666 A full implementation comprising all models and configuration files is available at <https://URL>.
667668 A.2 SANITY CHECK: SHUFFLED RANDOM LABELS
669670 To validate that the observed increase of generalization actually stems from the mitigated memo- 671 rization and is not a mere artifact, e.g., caused by effects on the scale of the feature activations, we 672 perform a simple sanity check. We reshuffle all random labels in each epoch. Thus, the random labels 673 cannot be learned and cannot serve as a metric for memorization. Consequently, the RLP-regularizer 674 also does not explicitly reduce the memorization, while all other implicit effects of the regularizer 675 remain. Results compared to our initially proposed RLP-regularization are shown in Figure A.1. As 676 expected, the random label accuracy remains approximately at the chance of random guessing $1/n$. The 677 train accuracy exhibits only a minor drop for high regularization factors. The test accuracy does 678 not improve and is only affected by high regularization factors where the performance drops. This 679 validates that the observed regularization is an effect of the mitigated memorization.
680681
682 Figure A.1: ViT-B/32 on ImageNet. As a sanity check we compare the regularization results for fixed 683 random labels (as before) to random labels shuffled in each epoch.
684693 A.3 ViT ON CIFAR-100
694695 In section 5.3, we found opposing effects caused by memorization mitigation for our two experiments 696 performed with ViT on ImageNet and with WideResNet on CIFAR-100. To clarify if the two ob- 697 served effects are caused by the different model architectures or datasets, we perform an additional 698 experiment where we study a ViT-S/4 trained on CIFAR-100. Results are shown in Figure A.2. Mem- 699 orization is effectively stopped for regularization factors $\lambda > 10^{-1}$. Similarly to our experiments with 700 WideResNet on CIFAR-100, we observe a detrimental effect of reducing memorization (unaffected 701 training accuracy and reduced test accuracy) indicating the dataset to be pivotal for the different 702 effects of memorization as we further examine in section 5.4.
703



714 A.4 NUMBER OF RANDOM LABELS

717 In Figure A.3 we analyze the effect of the number of different random labels n when using a linear
718 RLP-head. The input to the random prediction head, i.e., the feature dimension, stays constant
719 and since the output of the linear layer is given by the number of random labels n , the capacity of
720 the prediction head is directly tied to the number of random labels. Two intuitive implications can
721 be directly observed from Figure A.3: The probability to reach high values by chance decreases
722 with increasing n , i.e., the task to predict the random labels gets harder, and the capacity of the
723 RLP-head grows with increasing n , i.e., the capability of the RLP-head to solve the given task
724 increases. As a result, the reached random label accuracy undergoes a minimum before it approaches
725 full memorization and saturates. From this experiment, we conclude that the number of random
726 labels must be sufficiently large to ensure that the RLP-head has enough capacity to measure the
727 models memorization. However, increasing the number of random labels n also substantially raises
728 computational costs. Balancing these considerations, we set $n = 10,000$ for WideResNet experiments
729 on CIFAR-100 and $n = 100,000$ for ViT experiments on ImageNet.
730 To further validate our design choice on ImageNet, we additionally study the case where each training
731 sample is assigned a unique random label (i.e., $n = m = 1,281,167$), and analyze the resulting effect
732 of RLP-regularization in Appendix A.5.



742 Figure A.3: Linear RLP-head. A sufficiently large number of random labels n and thus head size
743 has to be chosen. **A:** WRN16-4 on CIFAR-100. **B:** ViT-B/32 on ImageNet. The minimum is barely
744 observable because the data starts at $n = 256$.

748 A.5 UNIQUE LABEL PER SAMPLE

751 We compare our proposed random label formulation with the alternative of assigning a unique label to
752 each sample. While the latter is computationally very expensive, it provides a direct measure of single-
753 sample memorization. As shown in Figure A.4, unique labels yield higher memorization accuracy,
754 due to the increased predictive capacity of the linear RLP-head. However, we observe no qualitative
755 differences compared to our proposed approach with $n = 100,000$ labels. For computational
efficiency, we adopt the latter approach in our experiments.

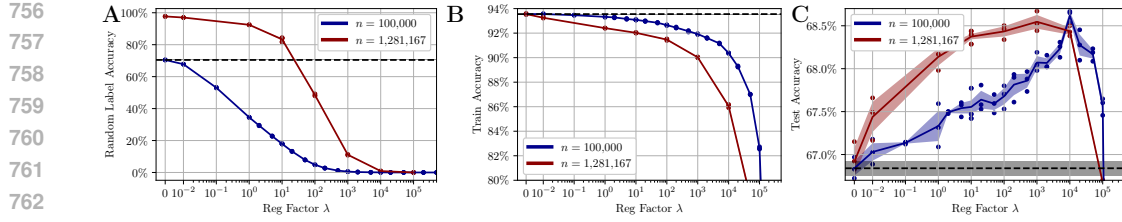


Figure A.4: ViT-B/32 on ImageNet. Using a unique label per sample when applying RLP-regularization (i.e., $n = m = 1,281,167$) compared to $n = 100,000$ used in the main paper.

A.6 TWO-LAYER HEAD

As shown in the last section (Appendix A.4) the RLP-head capacity and the number of random labels n are tied together for a linear head. To disentangle these two effects, we extend the RLP-head by adding a hidden fully-connected layer. We keep the number of labels constant at a rather small value in the experiment depicted in Figure A.5 ($n = 10$), and only influence the RLP-head capacity by varying its hidden feature dimension d_h . As can be seen, the RLP-head is now able to recover a much higher amount of random labels from the output of the corresponding feature extractor for a sufficiently large d_h , compared to the setting without a hidden layer in the RLP-head.

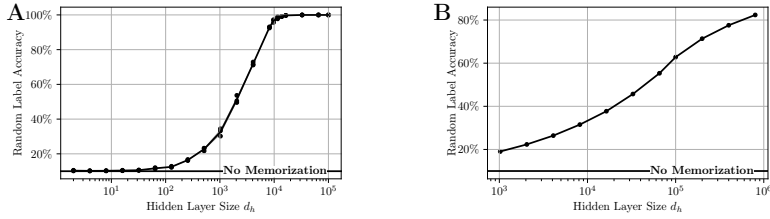


Figure A.5: A: WideResNet-16-4 on CIFAR-100. B: ViT-B/32 on ImageNet. RLP-head with one hidden layer. Number of random labels $n = 10$. Increasing the capacity of RLP-head leads to correctly predicted random labels.

Additionally, we do a sensitivity analysis on both the regularization strength controlled by λ and the hidden layer size d_h for WideResNet-16-4 on CIFAR-100. As shown in Figure A.6C small hidden layer dimensions have less impact on the test accuracy; however, the RLP-head is not capable to correctly predict the random labels under these conditions (see Figure A.6A). Larger RLP-heads do predict the random labels correctly and are thus sufficiently powerful to measure the network’s memorization, but are similarly detrimental to the models generalization. Adding a hidden layer to the RLP-head used for regularization neither improves generalization nor yields qualitatively new insights. We therefore use a linear RLP-head.

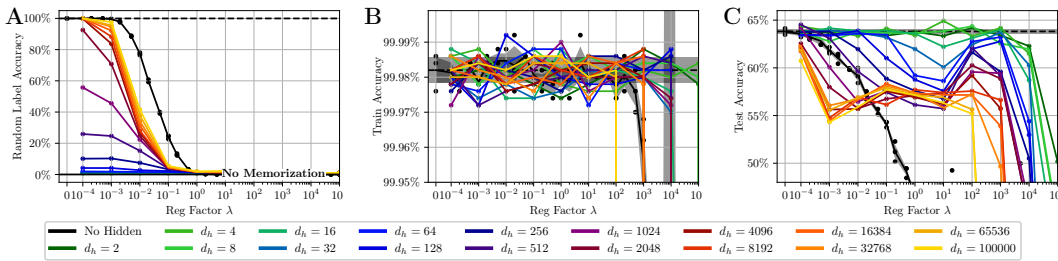
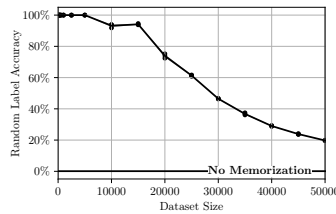


Figure A.6: WideResNet-16-4 on CIFAR-100. RLP-head with one hidden layer, $n = 100$.

810 A.7 DATASET SIZE
811

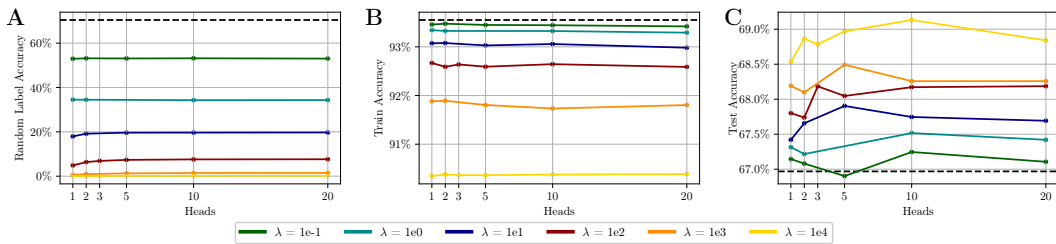
812 Having studied the influence of the RLP-head in previous sections (Appendix A.4 and Appendix A.6),
813 we aim to study the influence of the dataset size while maintaining the number of random labels and
814 the capacity of the RLP-head constant now. We thereby ablate the influence of the dataset size on the
815 difficulty of random label prediction task. We randomly sample subsets from CIFAR-100 in order
816 to construct several smaller datasets and use a small RLP-head with $n = 1024$. As shown in A.7,
817 the RLP-head is only able to predict the random labels correctly for small dataset sizes. Since we
818 showed before that a large RLP-head can reach 100 % random label accuracy on the full dataset, the
819 reduced random label accuracy is caused by the limited size of the RLP-head. We conclude from this
820 experiment, that the needed RLP-head size to obtain adequately measure the memorization in the
821 network grows with the dataset size.
822



830 Figure A.7: WideResNet-16-4 on CIFAR-100. Dependence of random label accuracy on the dataset
831 size for a small linear RLP-head of size $n = 1024$. The original dataset size of 50,000 training
832 samples of CIFAR-100 is reduced by sampling random subsets.
833

834
835 A.8 MULTI-HEAD RLP
836

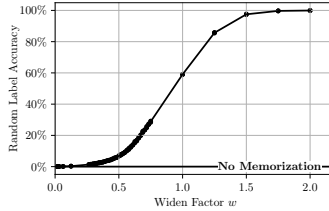
837 While we aim to measure single-sample memorization, we chose to generate a number of n random
838 labels for m total training samples, i.e., m/n samples per random label, where usually $n \ll m$.
839 For instance, we chose $n = 100,000$ for the $m = 1,281,167$ samples of ImageNet leading to
840 approx. 12 images which attain the same random label. This results in the RLP-regularizer to only
841 be able to effectively suppress features which are shared by parts of these random subsets of input
842 images. While setting $n = m$ (that is, learning an individual random label per sample) is studied in
843 Appendix A.5, this is not computationally feasible in practical scenarios. However, in the setting
844 $n \ll m$, it is harder for the RLP-head to identify sample-specific features (as opposed to those shared
845 in the random groups of images with the same random labels). This might allow the network to
846 memorize sample-specific features even though the RLP-regularizer is applied. To circumvent this
847 problem, we add multiple parallel RLP-heads receiving different sets of random labels. The total
848 regularization loss is the average of the individual regularization losses per RLP-head. This way, a
849 Multi-Head-RLP is developed which we hypothesize to be more powerful in identifying the networks
850 memorization. However, it is computationally more demanding. As shown in Figure A.8, the number
851 of heads in a multi-head setting does not impact the random label or train accuracy, but interestingly,
852 yields even higher test accuracy, reaching 69.2 % for 10 heads and $\lambda = 10^4$.
853



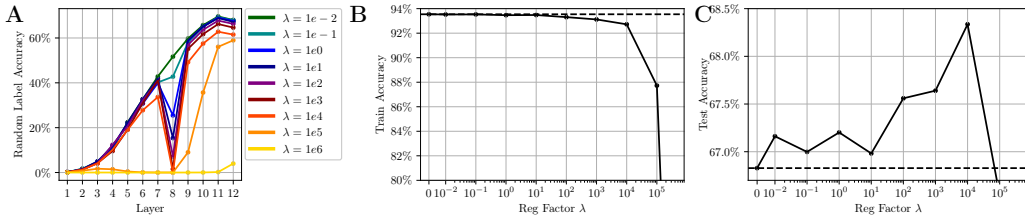
860 Figure A.8: ViT-B/32 on ImageNet. RLP-head used for regularization comprised of multiple parallel
861 linear layers, each receiving a different mapping from random labels to input images. The multi-head
862 structure results in improved generalization.
863

864 A.9 FEATURE EXTRACTOR SIZE
865

866 To validate the proposed random label accuracy as a capacity metric, we analyze the impact of
867 the feature extractor size on this measure. Specifically, we report the random label accuracy when
868 training WideResNet-16- w models with varying widening factors w on CIFAR-100, without applying
869 RLP-regularization (see Figure A.9). For small values of w , the models exhibit insufficient capacity
870 to fully memorize the training data, which is directly reflected in lower random label accuracy. As w
871 increases, the models progressively achieve higher random label accuracy, until reaching a plateau at
872 100 %, indicating complete memorization of the dataset. These results support the use of random label
873 accuracy, as measured by the RLP-head, as a reliable indicator of model capacity and complexity.
874

882 Figure A.9: WideResNet-16- w on CIFAR-100, $n = 10,000$.
883884 A.10 REGULARIZING INTERMEDIATE LAYERS
885

886 Our proposed RLP-regularizer enables control over memorization in a layer-selective manner. To
887 demonstrate this, we attach RLP-heads to all layers of a ViT trained on ImageNet (as in the main
888 paper’s section 5.5) to be able to monitor memorization across all layers, while we exclusively use the
889 RLP-head at layer 8 for regularizing the full feature extractor. As can be seen in Figure A.10, the effect
890 of the regularizer is highly localized: the random label accuracy at layer 8 is strongly suppressed,
891 approaching zero under large regularization strengths. In contrast, adjacent layers exhibit only minor
892 reductions in random label accuracy, and quickly recover beyond the regularized layer. Interestingly,
893 despite employing a single intermediate layer for regularization, the test accuracy improves to a degree
894 comparable to using RLP-regularization with the final layer, indicating enhanced generalization.
895

903 Figure A.10: ViT-B/32 on ImageNet. Only layer 8 is used for regularization.
904905 A.11 TEST-TRAIN DUPLICATES
906

907 Barz & Denzler (2020) show that CIFAR-100 contains numerous duplicates between the training
908 and test sets. This phenomenon provides a plausible explanation for the negative effect of the
909 RLP-regularizer’s memorization reduction on test performance: duplicated test samples implicitly
910 reward memorization of the training set. To address this issue, Barz & Denzler (2020) introduce a
911 de-duplicated variant, ciFAIR-100, in which all duplicated test images are replaced by newly sampled
912 datapoints.

913 We evaluate the RLP-regularizer in CIFAR-100 vs ciFAIR100 in Figure A.11. While the random label
914 accuracy and training accuracy remain similar across the two datasets, the reduction in memorization
915 induced by the RLP-regularizer is less detrimental on the train accuracy on ciFAIR-100 than on
916 CIFAR-100. This indicates that the degraded generalization performance observed on CIFAR-100 is,
917 at least in part, driven by train-test duplicates. Overall, this experiment further demonstrates that the
918 proposed RLP metric and regularizer are effective tools for analyzing memorization phenomena.

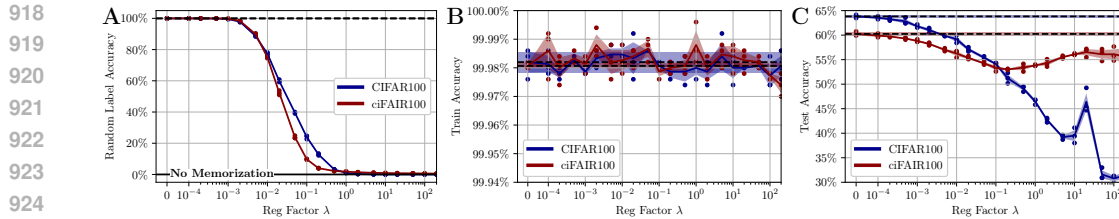


Figure A.11: WideResNet-16-4 on CIFAR-100 and ciFAIR100 (Barz & Denzler, 2020). Random label (A) train (B) and test (C) accuracy under RLP-regularization for different regularization factors λ .

A.12 FELDMAN SCORES

We compare the random label accuracy as a measure of memorization to the memorization score proposed by Feldman & Zhang (2020).

Feldman & Zhang (2020) define memorization per sample by testing whether a model needs to be trained on a specific sample in order to correctly classify it. Concretely, they consider the change in a model’s accuracy on each training dataset when the sample is either included in or excluded from the training set. Since an exact evaluation of this metric necessitates a full training run for each sample, the authors approximate it by removing 30 % of the training data at once and averaging results over multiple subsampled training runs to obtain a per-sample score. Even with this approximation, hundreds to thousands of full training runs are required. The resulting scores for ResNet-50 trained on CIFAR-100 are publicly available.

To compare against this method, we compute the random-label prediction accuracy per sample by averaging over 50 independently initialized training runs. Figure A.12 shows the distributions of the original Feldman scores, our reimplementation of their method, and random-label accuracy on CIFAR-100. The distributions differ clearly: the Feldman scores are bimodal, whereas the random-label accuracy is approximately Gaussian. Moreover, we find low correlation between the two measures (Pearson’s $r = 0.08$ with $p < 10^{-8}$).

Despite this, we validate that the random label accuracy is highly sample-specific. We performed an Anderson–Darling test to reject the hypothesis that all samples share the same underlying distribution, and repeated independent estimates of random-label accuracy per sample exhibit high correlation (Pearson’s $r \approx 0.9$). This confirms that random-label accuracy is indeed a stable property of each sample.

Although the lack of correlation between the two measures is counterintuitive, we argue that it is consistent with the previously observed lack of correlation between memorization and generalization for CIFAR-100.

Rather than directly measuring memorization, the Feldman score effectively measures whether the model can correctly classify a sample without having seen it, i.e., whether the model can generalize from the rest of the training set to that sample. It can be interpreted as constructing a one-sample validation set and comparing the model’s performance on this sample to its performance on the training set. In this sense, the Feldman score directly measures generalization. It can also be viewed as quantifying the uniqueness of a sample within the dataset. For example, two very similar samples of the same class that are distinct from the rest of the dataset (similar to duplicates found between test and train sets by Barz & Denzler (2020) discussed in Appendix A.11) will not receive a high Feldman score even if these samples are memorized.

In contrast, generalization does not affect the random label accuracy due to the non-existent correlation between label and sample, thus providing a measure of memorization independent of a possible link between memorization and generalization. The random label accuracy measures whether memorization occurs, irrespective of whether that memorization is beneficial.

Thus, the initially surprising lack of correlation between random label accuracy and the Feldman scores in fact supports the hypothesis that reduced memorization and improved generalization are not directly coupled.

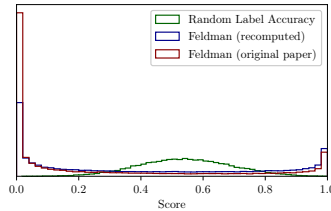
972
973
974
975
976
977
978

Figure A.12: Distribution of memorization scores proposed by Feldman & Zhang (2020) and distribution of per-sample random label accuracy on CIFAR-100. The original data from Feldman & Zhang (2020) were computed for ResNet-50, whereas our recomputed scores and random-label accuracy were derived using WideResNet-16-4.

A.13 NOISY LABELS

To further analyze the effects of RLP-regularization on memorization, we examine the training accuracy on randomly labeled samples within the training dataset. These datapoints can only be predicted correctly through memorization. As shown in Figure A.13, the RLP-regularizer reduces the training accuracy on samples with noisy labels, while the accuracy on samples with intact labels remains high even for large regularization strengths. The proposed regularizer thus targets memorized samples specifically. This is particularly true for $\lambda = 10^5$, where at the same time the test accuracy simultaneously reaches its maximum. By limiting the memorization of incorrectly labeled examples, the generalization gap is reduced. This experiment highlights the strong connection between the random label accuracy of the RLP-head and training performance on noisy labels, as well as the effectiveness of the RLP-regularizer in mitigating memorization of noisy labels.

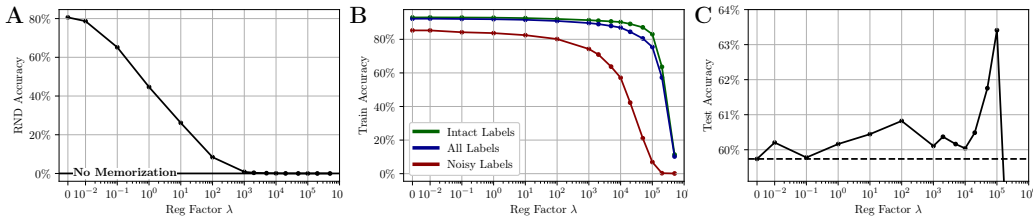


Figure A.13: ViT-B/32 on ImageNet with 10 % label noise. Random label accuracy (A), train accuracy (B), and test accuracy (C) for increasing regularization factors λ .

A.14 MEMORIZATION UNDER OTHER REGULARIZERS

We compare the effectiveness of the random label accuracy as a measure of memorization against the more direct approach of measuring memorization via training accuracy on noisy labels. We conduct this comparison under several common regularizers: label smoothing (Figure A.14), dropout (Figure A.15), and weight decay (Figure A.16). Consistent with our observations in section 5.2, all regularizers lead to reduced random label accuracy, supporting the validity of this metric as an indicator of network complexity. At the same time, the random label accuracy proves to be a reliable measure of memorization when compared with the training accuracy on noisy-labeled datapoints. Our proposed memorization measure is fully non-intrusive and can be applied without altering the training data, unlike noisy label injection.

Comparing these results with those obtained when the RLP-regularizer is applied (shown for the same training setup in Figure A.13), we observe similar improvements in test performance. However, the primary purpose of the RLP-regularizer is not to specifically improve generalization, but to explicitly control memorization in order to study and better understand its underlying mechanisms and identify when and where reducing memorization leads to improved generalization. While other regularizers also reduce memorization effectively (e.g., weight decay, which drives both random label accuracy and noisy label training accuracy close to 0%, as seen in Figure A.16), the RLP-regularizer allows targeted application to arbitrary layers. This makes it particularly well-suited for studying the evolution of memorization within the network, as e.g. explored in section 5.5.

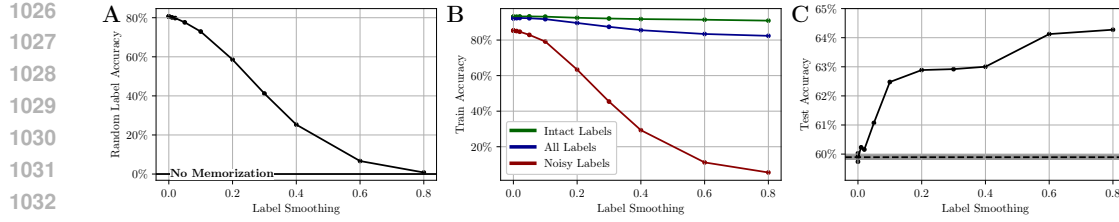


Figure A.14: ViT-B/32 on ImageNet with 10 % label noise and varying label smoothing strength.

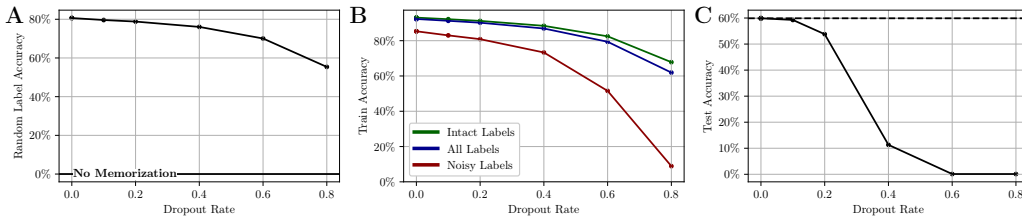


Figure A.15: ViT-B/32 on ImageNet with 10 % label noise and varying dropout strength.

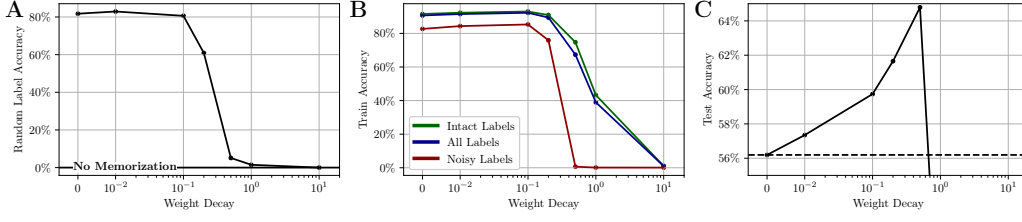


Figure A.16: ViT-B/32 on ImageNet with 10 % label noise and varying weight decay strength.

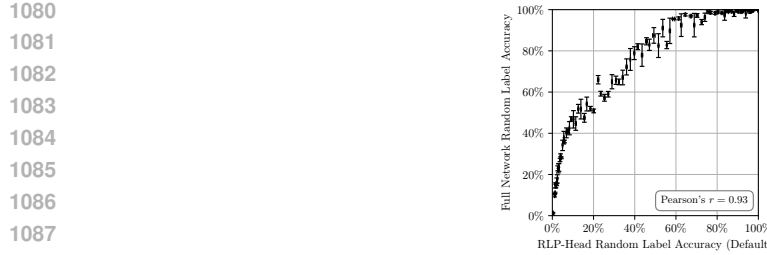
A.15 FULL NETWORK RANDOM TRAINING

To further support the connection between the random label accuracy as an empirical memorization measure and Rademacher complexity, we compare the random label accuracy of the proposed RLP-head with the training accuracy achieved when training an entire network on random labels across varying network widths.

The training accuracy obtained under fully random labels closely resembles the Rademacher complexity. The only approximations involved include using SGD to obtain an approximately optimal model instead of taking the supremum over all models, extending the binary-label definition to a multi-class accuracy setting, and estimating the expectation over random labelings via a finite number of independent training runs.

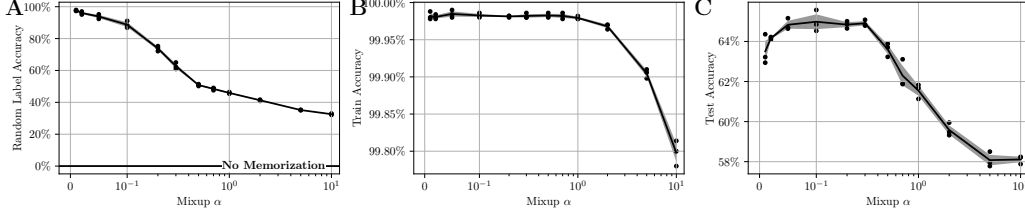
When varying the width of a WideResNet-16- w , we observe a strong correlation between the performance on random labels when the full network is trained end-to-end on these labels and the random label accuracy measured using the RLP-head only while the main network is trained on correctly labeled data as done in the rest of this manuscript.

This comparison also demonstrates that the random-label accuracy of the RLP-head is primarily determined by the capacity of the feature extraction network, rather than by the capacity of the head itself as long as the RLP-head is chosen to be sufficiently large.



A.16 MEMORIZATION WITH MIXUP

We evaluate the effect of mixup (Zhang et al., 2018b) on the random label accuracy. To do so, we apply mixup to the input images, class labels, and random labels during training, and then perform an additional epoch on the training set without mixup and without updating the weights in order to measure both the training accuracy and the random label accuracy. Since mixup is intended to reduce memorization, increasing the mixup strength (i.e., larger α) indeed lowers the random-label accuracy. However, we still observe substantial memorization even at $\alpha = 10$.



A.17 ADVERSARIAL ROBUSTNESS

We evaluated the adversarial robustness of a ViT-B/32 trained on ImageNet with the RLP-regularizer under attacks by PGD (Madry et al., 2018), FGSM Goodfellow et al. (2018) and APGDT Croce & Hein (2020). We used default hyperparameters and $\sigma = 0.1$ for gaussian noise and $\epsilon = 1/255$ for the other attack methods. We report results for the difference of the accuracy under attack to the baseline (i.e., no RLP-regularizer; $\lambda = 0$) for various regularization factors λ in Figure A.19 and the exact accuracies under attack for optimal $\lambda = 10^4$ in Table A.1. The RLP-regularizer improves the adversarial robustness in all scenarios.

Table A.1: Accuracy under adversarial attack of RLP-regularized models.

	Gaussian Noise	PGD	FGSM	APGDT
baseline ($\lambda = 0$)	25.1 ± 0.3	16.6 ± 0.2	23.4 ± 0.3	17.6 ± 0.2
RLP-regularized ($\lambda = 10^4$)	26.2 ± 0.8	18.0 ± 0.4	24.9 ± 0.5	18.5 ± 0.4

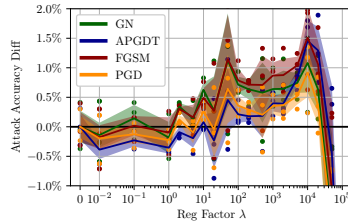


Figure A.19: Accuracy difference of RLP-regularized models to unregularized models under adversarial attacks.

A.18 MEMBERSHIP INFERENCE ATTACKS

We perform membership inference attacks on our ViT-B/32 trained on ImageNet to assess if the RLP-regularizer leads to improved membership robustness. We use an MLP with 2 hidden layers (dimensions 512 and 256) to perform binary classification on the sorted logits of the models to determine if a sample was part of the training data or not. We train our attack model on the logits of the original model and create a balanced test dataset to evaluate the accuracy of the membership prediction. The attack model is trained for 10 epochs using the Adam optimizer with a learning rate of 10^4 and a batch size of 256. We evaluate three independently initialized ViT models attacked by five independently initialized attack models each. While the model is not very vulnerable to membership inference attacks without RLP-regularization ($64.27\% \pm 0.05\%$), the RLP-regularizer further increases the robustness of the model reducing the membership accuracy to $62.27\% \pm 0.06\%$ for the regularization factor of optimal generalization $\lambda = 10^4$. Full results are reported in Figure A.20.

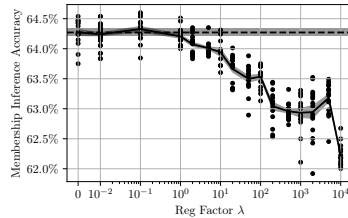


Figure A.20: Membership Inference Accuracy for ViT-B/32 models trained under RLP-regularization.

A.19 MEMORIZATION OF LONG-TAIL SAMPLES

To test our hypothesis that memorization is beneficial for undersampled data distributions but not for sufficiently sampled ones, we conduct an additional experiment using a ViT-B/32 model trained on the ImageNet-LT (long-tail) dataset Liu et al. (2019b). ImageNet-LT is a subset of the original ImageNet dataset in which certain classes are deliberately undersampled in the training set, while the test set remains unchanged.

We compare test performance as a function of the number of training samples per class, evaluating models trained with and without RLP-regularization in Figure A.21. Under RLP-regularization, where memorization is stopped, lower test performance is reached for classes with low sample counts, i.e. classes with fewer than 80 training samples are not learned. For classes with higher sample counts, performance sometimes improves and sometimes does not.

These results support our hypothesis that memorization is useful in undersampled regimes and may or may not be in oversampled regimes.

1188

1189

1190

1191

1192

1193

1194

1195

Figure A.21: ViT-B/32 trained for 300 epochs on ImageNet-LT without RLP-regularizer and with regularizer ($\lambda = 10^5$). Average test accuracy per class count.

1196

1197

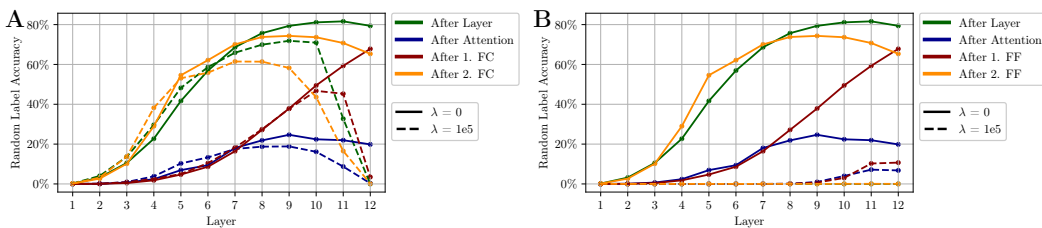
A.20 RLP-HEADS INSIDE TRANSFORMER LAYERS

To test our hypothesis that memorization is shifted into the transformer blocks under RLP-regularization applied to the output of all transformer blocks, we insert additional RLP-heads inside the transformer blocks: after the attention mechanism, after the first fully connected layer, and after the second fully connected layer of each transformer block. The corresponding results are shown in Figure A.22.

Although all additional heads detect memorization within the network, the largest values still appear at the output of each transformer block as measured in the rest of this manuscript. When applying RLP-regularization only to the final block head, memorization is reduced in the components of later transformer blocks, as illustrated in Figure A.22A.

However, when regularizing based on all RLP-heads, as in Figure 8B, we observe non-zero memorization in the last four transformer blocks after the attention mechanism and after the first fully connected layer (see Figure A.22B). Additional memorization may also be encoded within the representations inside the attention mechanism itself.

1213



1221

1222

1223

1224

1225

A.21 FROZEN FEATURE EXTRACTOR AFTER REGULARIZATION

1226

1227

1228

1229

1230

1231

1232

1233

1234

1235

1236

1237

1238

1239

1240

1241

Figure A.22: Random label accuracy inside transformer blocks. **A:** Regularization based on the RLP-head attached after block 12 only. **B:** Regularization based on the RLP-heads attached after all blocks.

A.21 FROZEN FEATURE EXTRACTOR AFTER REGULARIZATION

To verify that memorization is genuinely mitigated by the RLP regularizer—and not merely concealed from the specific RLP-head trained alongside it, we conducted an additional experiment using our ViT-B/32 setup on ImageNet. We train a new RLP-head as before, but keep the feature extractor frozen using the weights obtained from a previous training run with RLP-regularization (in the default setup). This setup tests whether a newly trained RLP-head can recover the random labels using the representations learned under regularization. Importantly, the random-label mapping between samples remains unchanged across the two runs. With a regularization strength of $\lambda = 10^{-4}$ applied during training of the feature extractor, the newly trained RLP-head achieves a random label accuracy of only 2.9 %. This provides further evidence that the RLP-regularizer effectively mitigates memorization rather than merely obscuring it.

A.22 TEXT CLASSIFICATION

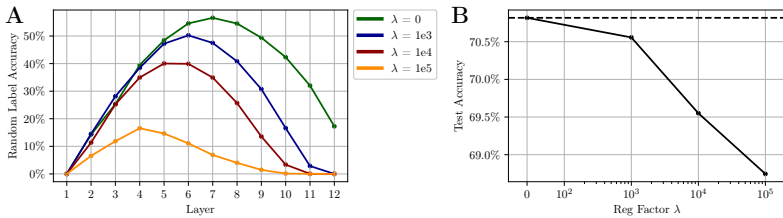
We use the RLP-heads to study memorization in language tasks. Our experiments are conducted on Yahoo! Answers (Zhang & LeCun, 2016) using RoBERTa-base (Liu et al., 2019a) trained with Adam and a learning rate of $2 \cdot 10^{-5}$ with cosine scheduling for 50 epochs. Results are shown in Figure A.23.

1242 Interestingly, without regularization we observe pronounced memorization in the early layers, peaking
 1243 at layer 7 and decreasing in later layers. This suggests that the model may be oversized for the given
 1244 dataset.

1245 While RLP-regularization applied via the RLP-head on the final (12th) transformer layer reduces
 1246 memorization across all layers, we do not observe a shift of memorization towards later layers unlike
 1247 the ViT results on ImageNet shown in Figure 8.

1248 Furthermore, test accuracy does not improve with RLP-regularization, indicating that memorization
 1249 may actually benefit generalization for the studied model and dataset.

1250



1258 Figure A.23: RoBERTa-base trained on Yahoo! Answers with RLP-regularization based on the
 1259 RLP-head attached to the final (12th) transformer layer only. **A:** Random label accuracy of RLP-heads
 1260 at different layers. Memorization occurs in early layers and is reduced in later layers. **B:** The test
 1261 accuracy does not improve when memorization is suppressed.

1262

1263

1264

1265

1266

1267

1268

1269

1270

1271

1272

1273

1274

1275

1276

1277

1278

1279

1280

1281

1282

1283

1284

1285

1286

1287

1288

1289

1290

1291

1292

1293

1294

1295